Biatrial Modelling for In Silico Prediction of Atrial Fibrillation Inducibility

Semhar B Misghina[1], Jose A Solis-Lemus[2], Edward J Vigmond [3], Steven A Niederer[2], Caroline H Roney[1]

[1]Queen Mary University of London, London, United Kingdom
[2]Imperial College London, London, United Kingdom
[3]University of Bordeaux, Bordeaux, France

Abstract

Atrial fibrillation (AF) is a cardiac disorder characterised by rapid atrial contractions. Current treatments, including ablation, vary in effectiveness. Recent mechanistic modelling studies have highlighted the significance of the right atrium (RA) in predicting AF outcomes, although its role remains unclear. This study employs a novel open-source biatrial modelling pipeline to assess AF inducibility and monitor AF dynamics on clinical timescales.

Patient-specific models were created from late gadolinium enhancement MRI (LGE-MRI) scans of 20 patients. Manual RA and left atrial (LA) segmentation, fibrosis mapping in pre-processing, and calculation of atrial coordinates to incorporate atrial structures and fibres were performed. These personalised models were simulated and post-processed to assess the AF wavefront patterns.

RA integration significantly increased rotor activity and total phase singularities (PS) within the LA posterior walls and reduced conduction velocity, indicating greater potential for AF sustainability. LA exhibited a higher mean PS density (3.8 rotors/cm²) than RA (2.1 rotors/cm²), indicating regions prone to re-entry or wavefront break-up.

The modelling pipeline highlights the potential of biatrial models to efficiently predict AF outcomes, enabling personalised therapies and comparisons of ablation approaches and anti-arrhythmic drug therapies.

1. Introduction

Atrial fibrillation (AF) is a prevalent cardiac arrhythmia characterised by abnormal electrical impulses [1]. Current anti-arrhythmic drugs are suboptimal, making radiofrequency catheter ablation (RFCA) the gold standard [1]. RFCA poses challenges in predicting ablation targets, leading to the adoption of LGE-MRI for 3D mapping and optimised therapy. These imaging advances enhance personalised therapy and streamline clinical workflows. [2].

Prior research has primarily focussed on LA modelling to understand AF; however, the potential of biatrial models in predicting AF inducibility remains underexplored [3,4]. RA presents challenges due to limited pre-labelled datasets and geometric variability, especially in manual segmentation [2]. This study addresses these constraints as cardiac modelling advances towards large-scale in silico studies and personalised predictions, which holds potential for patient-specific and population digital twins [3,4].

We present a biatrial modelling pipeline using LGE-MRI data from 20 patients. To address RA segmentation challenges, we employed segmentation tools with an MRI atlas. Patient-specific bilayer meshes incorporated atrial fibres and structures from a fibre atlas using atrial coordinates. We conducted finite element simulations and evaluated PS density maps for AF inducibility assessment.

2. Materials and Methods

2.1. Patient Cohort

This study used LGE-MRI scans of the atria from 20 patients in the Atrial Segmentation Challenge Dataset (2018) [5]. These scans had a spatial resolution of 0.625 x 0.625 x 0.625 mm³ with variable spatial dimensions (576 x 576 x 88 or 640 x 640 x 88 pixels). Ethical guidelines were followed, and all patients provided informed consent [6].

2.2. Image Segmentation

Atrial anatomical models were created from LGE-MRI data using 3D Slicer software (version 5.3.0). This process involved importing DICOM data, manually tracing LA and RA from individual 2D cross-sectional images, and exporting 3D models in NIfTI format for mesh pre-processing. To ensure accurate labelling, pre-labelled LA datasets and a reference MRI atlas were employed, validated by a cardiac modelling expert. Segmented meshes were saved in the VTK file format for all cases. All the steps in the model construction process are shown in Figure 1.

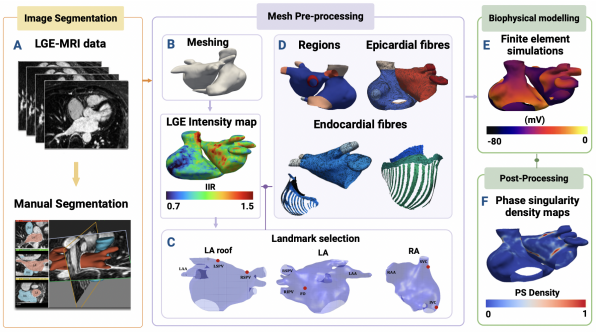

Figure 1. **Model development and AF simulation protocol.** (A) LGE-MRI data acquisition and manual segmentation, mesh pre-processing with (B) LGE intensity registration, and (C) region assignment using landmark selection. (D) Integration of atrial fibres from the Labarthe et al.(2014) atlas with atrial coordinates, depicting endocardial fibres as streamlines. (E) Finite element simulations for AF induction and (F) subsequent post-processing. (LA regions: LA body (dark blue), left superior pulmonary vein (yellow), left atrial appendage (grey), right superior pulmonary vein (dark orange), right inferior pulmonary vein (red), left inferior pulmonary vein (orange). RA regions: RA body (dark blue), superior vena cava (light grey), inferior vena cava (orange) and coronary sinus (grey)).

2.3. Mesh Pre-processing

The subsequent steps form a mesh for electrophysiological modelling. The LA and RA models were imported into the CemrgApp software (v2.2.1) to project the maximum LGE intensities onto the meshes [7]. A predefined image intensity ratio (IIR), which normalises pixel intensity on the atrial wall by mean blood pool intensity, classified regions as normal (IIR $<$1.22) or scarred (IIR $>$1.22) [3, 8]. Closed surface meshes were clipped at the pulmonary veins (PVs), mitral valve (MV), coronary sinus (CS), tricuspid valve (TV), and vena cava (VC) using Paraview software (v5.9.0) [3].

2.4. Landmark Selection

We employed a rule-based approach with a custom MATLAB script to define both general and specific regions while establishing boundary conditions [9]. In the LA, general landmarks included the right superior pulmonary vein (RSPV), left superior pulmonary vein (LSPV), right inferior pulmonary vein (RIPV), left inferior pulmonary vein (LIPV), and left atrial appendage (LAA) apex. Specific landmarks were assigned at the highest lateral positions, LSPV-LA and RSPV-LA body intersections, and the lateral-septal border parallel to LSPV and RSPV. In the RA, general landmarks included the right atrial appendage (RAA) apex, coronary sinus, inferior vena cava (IVC), and superior vena cava (SVC) [3]. Specific landmarks were placed at the SVC-RA and IVC-RA body intersections, corresponding to the highest lateral positions, and aligned with the SVC and IVC at the lateral-septal confluence [9].

Subsequently, Laplace-Dirichlet solves in openCARP cardiac electrophysiology simulation software were performed to automatically identify atrial regions (PV, VC, LAA, RAA, and CS), and universal atrial coordinates (UAC) were calculated using previous methods [2].

2.5. Fibre Modelling

Patient-specific surface meshes were used to construct the atrial coordinates. These coordinates integrated atrial structures and fibres from Labarthe et al.(2014) atlas, including endocardial and epicardial fibres, pectinate muscles (PM), cristae terminalis (CT), Bachmann's bundle (BB) and the sino-atrial node (SAN) [2, 9]. The resulting bilayer models included interatrial pathways [2].

2.6. Biophysical Modelling

Biophysical simulations used the human atrial ionic model of Courtemanche et al.(1999) and a monodomain solver within openCARP for excitation propagation [10]. The ionic model parameters were adjusted to represent persistent AF remodelling and repolarisation variability [3]. AF was induced following Roney et al.(2020) method, initiating AF with initial parameters associated with four spiral wave re-entries [3, 9]. Post-processing detected total PSs, PS hotspots, and changes in rotor activity [3].

3. Results

3.1. Segmented Cohort

The atria, including PV, CS, VC, MV, LAA, and TV, were manually segmented using 3D Slicer. Figure 2 displays LA and RA geometries of 20 individuals, highlighting their morphological diversity. Challenges in segmenting the LAA and MV arose from unclear LA-LV boundaries and poor image contrast, leading to some labelling disparities.

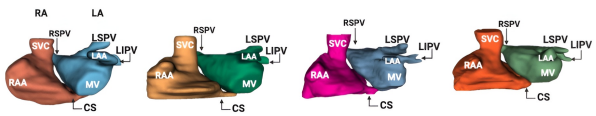

Figure 2. **3D representations of the segmented anatomies of the LA and RA in the anteroposterior (AP) view.** LA regions: LSPV, RSPV, LAA, and LIPV. RA regions: SVC, IVC, CS, and RAA.

3.2. Fibrotic Remodelling

Fibrotic modelling, based on LGE intensities, revealed significant diversity among the 20 anatomies, as shown in Figure 3A. Models that required corrections in clipping and segmentation were revised, and an example clipping is shown in Figure 3B. The diverse atrial geometry posed challenges in landmark selection, but expert validation ensured accuracy. The meshes were combined to create biatrial models, which were validated visually and by fibre mapping, with two excluded due to insufficient segmentation.

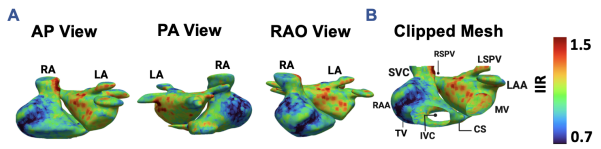

Figure 3. **LGE intensities projected on the 3D LA and RA meshes to incorporate fibrosis.** (A) Fibrosis mapping showing healthy (blue) and scarred tissue (red) in the AP, posteroanterior (PA), and right atrial oblique (RAO) views. The colour axis indicates the IIR values. (B) Clipped LA and RA surfaces at PV, CS, VC, TV, and MV.

3.3. Fibre Modelling

Our approach, similar to Roney et al.(2022) methods, maps atrial structures and fibres in both the LA and RA [3]. Figure 4 shows fibre configurations in the biatrial models, highlighting their significance in personalisation. The exclusion of complex atrial meshes streamlined fibre integration, facilitating biophysical modelling.

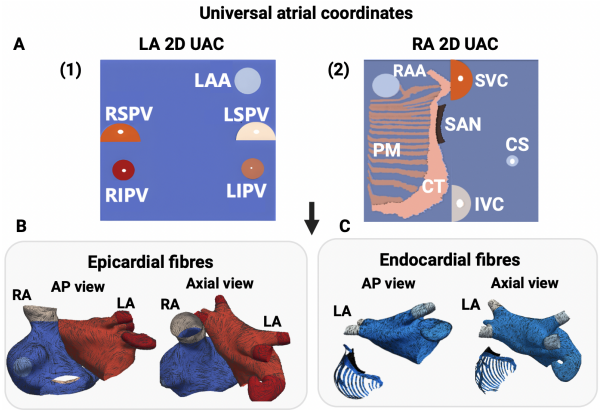

Figure 4. **Atrial fibres from Labarthe et al.(2014) atlas were modelled using 2D UAC systems for the (1) LA and (2) RA.** (B) Epicardial and (C) endocardial surfaces are depicted in AP and axial views as streamlines. [2]

3.4. Biophysical Models

Finite element simulations assessed AF dynamics over 15 s in a biatrial model. Figure 5 shows slower conduction in the LA posterior walls (LAPW), indicating significantly slower mean conduction velocity in the LA (31.7 cm/s) than in the RA (48.2 cm/s).

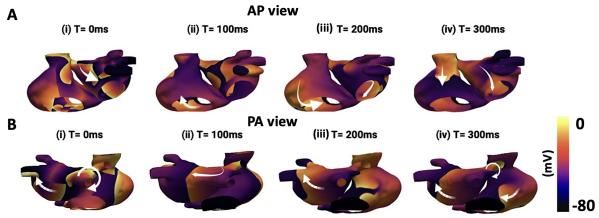

Figure 5. **Transmembrane potential maps from AF simulations using openCARP software depict AF induction at 0ms, 100ms, 200ms, and 300ms.** Arrows indicate wavefront patterns in (A) AP and (B) PA views, with the colour bar showing transmembrane potential in mV.

Figure 6 shows PS density maps with increased rotor activity and PS hotspots in the LAPW, suggesting re-entry prone areas and a higher likelihood of sustained AF. The LA exhibits a maximal phase singularity density of 3.8 rotors/cm^2, while the RA has 2.1 rotors/cm^2.

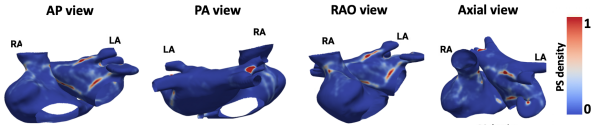

Figure 6. **Post-processed PS density maps from AF simulations are shown in AP, PA, axial, and RAO views.** These maps show PS hotspot localisation in the LAPW.

4. Discussion

In this study, we developed biatrial models using LGE-MRI data to predict AF inducibility in 20 patients. Rotors, functional re-entry mechanisms in AF, are influenced by ionic variations and scarring. Integrating RA significantly affected AF dynamics, with PS density maps indicating increased rotor activities in the LAPW, which are markers of AF recurrence. These rotor locations were aligned with regions of scar tissue identified during mesh pre-processing.

Our biatrial modelling aligns with Calo et al.(2006) findings, highlighting the key role of RA re-entrant arrhythmias in AF development and ablation treatment. These studies also identified conduction issues and chaotic impulses in certain atrial walls [11]. Our work extends the study of Nagel et al.(2021) , which focussed on biatrial statistical modelling and imaging metrics for assessing AF

activity. This study assesses AF dynamics using patient-specific biatrial models and expands the literature on the role of RA in AF recurrence, complementing Hopman et al.(2023) work on RA fibrotic remodelling and ablation approaches [4, 12]. This study assesses the specific effects of RA and LA on AF recurrence, potentially informing personalised catheter ablation strategies.

The biatrial modelling framework has limitations, particularly in manual segmentation, introducing intra-operator variability. Although developing an autonomous biatrial modelling pipeline is not the focus of this study, it could minimise errors and enhance region assignment repeatability [13]. Although model personalisation is important in identifying AF trends, our biatrial models do not account for specific patient attributes such as comorbidities, limiting their applicability in diverse populations [3].

This study aimed to predict AF inducibility using biatrial models. It also offers the potential for assessing ablation strategies to treat AF recurrence. Future work will extend this work to the UK Biobank longitudinal dataset, enabling long-term post-AF treatment outcome prediction. Our objectives will address the challenges of inferring missing atrial longitudinal data, constructing models from low-resolution imaging data, and integrating ECG data using biophysical models and machine learning. These research directions advance our understanding of AF mechanisms and streamline clinical workflows.

5. Conclusion

Our study introduces a biatrial cohort to assess AF patterns and highlights the role of RA in predicting AF inducibility. These findings highlight the potential of biatrial substrates in the development of personalised patient-specific and population digital twins.

Acknowledgments

This research was funded by a UKRI Future Leaders Fellowship (MR/W004720/1).

References

[1] Pashakhanloo F. High-Resolution Whole-Heart Imaging and Modeling for Studying Cardiac Arrhythmia. Ph.D. thesis, Johns Hopkins University, 2016.

[2] Zhuang X. Automatic whole heart segmentation based on image registration. Ph.D. thesis, UCL (University College London), 2010.

[3] Roney CH, Sim I, Yu J, Beach M, Mehta A, Solis-Lemus JA, Kotadia I, Whitaker J, Corrado C, Razeghi O, et al. Predicting atrial fibrillation recurrence by combining population data and virtual cohorts of patient-specific left atrial models. Circulation Arrhythmia and Electrophysiology 2022;15(2):e010253.

[4] Hopman LH, Visch JE, Bhagirath P, van der Laan AM, Mulder MJ, Razeghi O, Kemme MJ, Niederer SA, Allaart CP, Götte MJ. Right atrial function and fibrosis in relation to successful atrial fibrillation ablation. European Heart Journal Cardiovascular Imaging 2023;24(3):336–345.

[5] Borra D, Andalò A, Paci M, Fabbri C, Corsi C. A fully automated left atrium segmentation approach from late gadolinium enhanced magnetic resonance imaging based on a convolutional neural network. Quantitative Imaging in Medicine and Surgery 2020;10(10):1894.

[6] McGann C, Kholmovski E, Blauer J, Vijayakumar S, Haslam T, Cates J, DiBella E, Burgon N, Wilson B, Alexander A, et al. Dark regions of no-reflow on late gadolinium enhancement magnetic resonance imaging result in scar formation after atrial fibrillation ablation. Journal of the American College of Cardiology 2011;58(2):177–185.

[7] Razeghi O, Solís-Lemus JA, Lee AW, Karim R, Corrado C, Roney CH, de Vecchi A, Niederer SA. Cemrgapp: An interactive medical imaging application with image processing, computer vision, and machine learning toolkits for cardiovascular research. SoftwareX 2020;12:100570.

[8] Gunturiz-Beltrán C, Borràs R, Alarcón F, Garre P, i Ventura RMF, Benito EM, Caixal G, Althoff TF, Tolosana JM, Arbelo E, et al. Quantification of right atrial fibrosis by cardiac magnetic resonance: verification of the method to standardize thresholds. Revista Espanola de Cardiologia English Edition 2023;76(3):173–182.

[9] Roney CH, Pashaei A, Meo M, Dubois R, Boyle PM, Trayanova NA, Cochet H, Niederer SA, Vigmond EJ. Universal atrial coordinates applied to visualisation, registration and construction of patient specific meshes. Medical image analysis 2019;55:65–75.

[10] Courtemanche M, Ramirez RJ, Nattel S. Ionic targets for drug therapy and atrial fibrillation-induced electrical remodeling: insights from a mathematical model. Cardiovascular research 1999;42(2):477–489.

[11] Calò L, Lamberti F, Loricchio ML, De Ruvo E, Colivicchi F, Bianconi L, Pandozi C, Santini M. Left atrial ablation versus biatrial ablation for persistent and permanent atrial fibrillation: a prospective and randomized study. Journal of the American College of Cardiology 2006;47(12):2504.

[12] Nagel C, Schuler S, Dössel O, Loewe A. A bi-atrial statistical shape model for large-scale in silico studies of human atria: model development and application to ecg simulations. Medical Image Analysis 2021;74:102210.

[13] Aguado AM, Olivares AL, Yagüe C, Silva E, Nuñez-García M, Fernandez-Quilez Á, Mill J, Genua I, Arzamendi D, De Potter T, et al. In silico optimization of left atrial appendage occluder implantation using interactive and modeling tools. Frontiers in physiology 2019;10:237.

Address for correspondence:

Semhar Misghina
Queen Mary University of London, UK
s.b.misghina@qmul.ac.uk